Preformed Cooper Pairs in Layered FeSe-Based Superconductors

B. L. Kang,[1] M. Z. Shi,[1] S. J. Li,[1] H. H. Wang,[1] Q. Zhang,[1] D. Zhao,[1] J. Li,[1] D. W. Song,[1] L. X. Zheng,[1] L. P. Nie,[1] T. Wu,[1,2,3,4,*] and X. H. Chen[1,2,3,4,†]

[1]*Hefei National Laboratory for Physical Sciences at the Microscale and Department of Physics, and Key Laboratory of Strongly-Coupled Quantum Matter Physics, Chinese Academy of Sciences, University of Science and Technology of China, Hefei, Anhui 230026, China*

[2]*CAS Center for Excellence in Superconducting Electronics (CENSE), Shanghai 200050, China*

[3]*CAS Center for Excellence in Quantum Information and Quantum Physics, Hefei, Anhui 230026, China*

[4]*Collaborative Innovation Center of Advanced Microstructures, Nanjing University, Nanjing 210093, China*

(Received 15 December 2019; revised 6 June 2020; accepted 27 July 2020; published 28 August 2020)

Superconductivity arises from two distinct quantum phenomena: electron pairing and long-range phase coherence. In conventional superconductors, the two quantum phenomena generally take place simultaneously, while in the underdoped high-T_c cuprate superconductors, the electron pairing occurs at higher temperature than the long-range phase coherence. Recently, whether electron pairing is also prior to long-range phase coherence in single-layer FeSe film on $SrTiO_3$ substrate is under debate. Here, by measuring Knight shift and nuclear spin-lattice relaxation rate, we unambiguously reveal a pseudogap behavior below $T_p \sim 60$ K in two kinds of layered FeSe-based superconductors with quasi2D nature. In the pseudogap regime, a weak diamagnetic signal and a remarkable Nernst effect are also observed, which indicates that the observed pseudogap behavior is related to superconducting fluctuations. These works confirm that strong phase fluctuation is an important character in the 2D iron-based superconductors as widely observed in high-T_c cuprate superconductors.

DOI: 10.1103/PhysRevLett.125.097003

Phase fluctuation is an important character for high-T_c superconductivity [1] and determines the condensation of Cooper pairs. In conventional Bardeen-Cooper-Schrieffer superconductors, the superfluid density is so large that the pairing and condensation of Cooper pairs always happen simultaneously, and the superconducting transition temperature (T_c) is determined by the pairing temperature (T_p). However, in the underdoped high-T_c cuprate superconductors, which were treated as a doped Mott insulator [2], the famous "Uemura relation" indicates a close correlation between the superfluid density and T_c [3], suggesting an important role of phase fluctuation in the determination of T_c [1]. Previous studies also observed significant superconducting fluctuations above T_c, supporting a preformed pairing scenario [4–7]. In contrast, the signature of preformed pairing in another high-T_c family, iron-based superconductors, remains elusive [8–13]. The discovery of large pairing gap in single-layer FeSe film on $SrTiO_3$ substrate sheds light on this issue [14]. The interface as a possible origin to enhance superconducting pairing in the single-layer FeSe film on $SrTiO_3$ has been widely discussed [15–21]. In addition, the angle-resolved photoemission spectroscopy experiments revealed that the closing temperature of the pairing gap in single-layer FeSe film is up to 65 K [22,23] while the zero-resistance transition temperature (T_{c0}) determined by transport measurement is mostly below 40 K [24–27]. A natural explanation of such phenomenon is related to the preformed pairing analogous to the case in underdoped cuprate superconductors.

Very recently, organic ion intercalated FeSe superconductors $(CTA)_xFeSe$ [28] and $(TBA)_xFeSe$ [29] with $T_{c0} \sim 43$ K have been synthesized. As shown in Fig. 1(a), the charge from organic ion tetrabutyl ammonium (TBA^+) is transferred to FeSe layers, which is important to achieve high-T_c superconductivity in FeSe layer [17,22,25,30]. The distance between adjacent FeSe layers is enlarged from ~5.5 Å in pristine FeSe to ~15.5 Å in $(TBA)_xFeSe$ due to the intercalation of TBA^+. The intercalation of organic ion makes the $(TBA)_xFeSe$ superconductor two dimensional (2D). In these 2D FeSe-based superconductors, we unambiguously reveal an intrinsic pseudogap behavior below $T_p \sim 60$ K by measuring Knight shift and nuclear spin-lattice relaxation rate. In addition, a weak 2D diamagnetic signal and a remarkable Nernst effect are also observed in the pseudogap regime. These results definitely verify the preformed Cooper pairs in the 2D FeSe-based superconductors, which should be the same scenario for the single-layer FeSe film.

Nuclear magnetic resonance (NMR) is a bulk-sensitive local probe to measure spin susceptibility (χ_s). When the electrons are bound into Cooper pairs with a spin-singlet pairing, the local spin susceptibility will diminish below pairing temperature. Even if the long-range coherence among Cooper pairs is lost due to strong phase fluctuations,

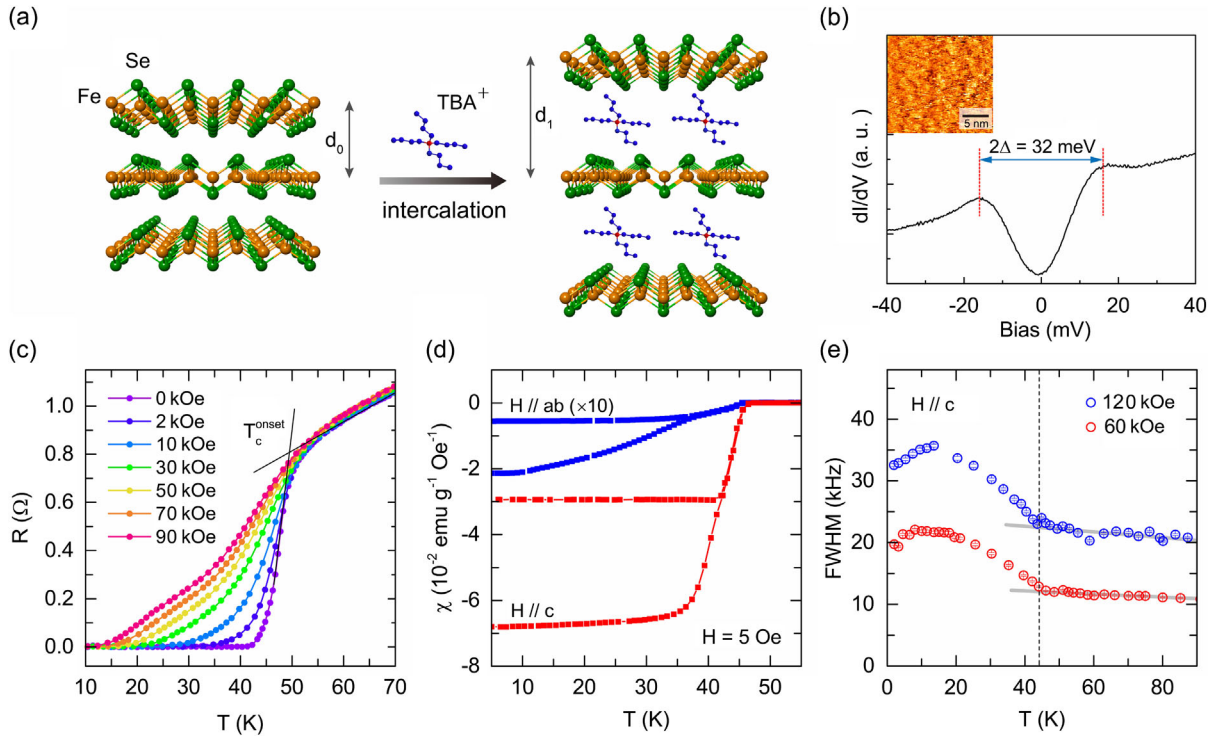

FIG. 1. Crystal structure and superconducting properties of $(TBA)_xFeSe$. (a) The crystal structure of pristine FeSe with c-axis lattice constant $d_0 \sim 5.5$ Å and the intercalated $(TBA)_xFeSe$ with $d_1 \sim 15.5$ Å. (b) Tunneling spectrum taken on a cleaved surface of $(TBA)_xFeSe$ at 5 K reveals the appearance of a superconducting gap. Pronounced superconducting coherence peaks appear at ± 16 meV. Inset: Atomically flat STM image for $(TBA)_xFeSe$ with a bias voltage of $V_{\text{bias}} = 1$ V and tunneling current of $I_t = 220$ pA. (c) Temperature dependence of in-plane resistance under different magnetic fields applied along c axis. The T_c^{onset} is determined by the intersection of the linear extrapolation of normal-state resistance R_n and the sharp superconducting transition, and the T_{c0} is determined by using the one percent normal state resistance criterion. The fan-shaped broadening of resistive transition under magnetic fields indicates a strong 2D characteristic. (d) Temperature dependence of anisotropic magnetic susceptibility measured in field-cooling and zero-field-cooling modes under magnetic field of 5 Oe applied along in plane (blue) and out of plane (red), respectively. The significant difference of shielding fraction between two orientations, usually up to dozens of times, supports a strong 2D characteristic. (e) Temperature dependent FWHM of ^{77}Se NMR spectra under different external magnetic fields. The temperature indicated by dashed line is defined as the superconducting transition temperature (T_c) in the H-T phase diagram of Fig. 4.

a drop in the local spin susceptibility is still expected [31]. In NMR measurements, both the Knight shift (K) and the nuclear spin-lattice relaxation rate ($1/T_1$) are related to the spin susceptibility. Usually, the Knight shift is related to the uniform spin susceptibility with $K_{\text{tot}} = A\chi_s + K_{\text{orb}}$, where K_{orb} is the orbital contribution and is always temperature independent, and A is the hyperfine coupling tensor between nuclear and electronic spins. The nuclear spin-lattice relaxation rate ($1/T_1$) is related to dynamic spin susceptibility with $1/T_1T \sim \Sigma_q \gamma_n^2 |A_\perp(q)|^2 (\chi''(q,\omega)/\omega)$, where $\chi''(q,\omega)$ is the q-dependent dynamic spin susceptibility and $A_\perp(q)$ is the transverse hyperfine form factor (see Supplemental Material [32], Section I, for more details). Usually, $1/T_1T = 1/T_1^{QP}T + 1/T_1^{SF}T$, in which the first term is from quasiparticles and the second is from additional spin fluctuations. In a Fermi liquid picture, which ignores the q-dependent spin fluctuations, both of the quantities keep a simple Korringa relation with $1/T_1T \sim K^2 \sim N(E_F)^2$ [80], where $N(E_F)$ is the density of state at Fermi level. In this sense, both Knight shift and nuclear spin-lattice relaxation rate are practical to identify pseudogap phenomenon [81] that leads to a suppression of $N(E_F)$.

As shown in Fig. 2(a), the temperature-dependent Knight shift of ^{77}Se nuclei shows a clear deviation from the high-temperature behavior below 60 K, which is more evident in the differential curve. If superconductivity is considered as the only active electronic instability at low temperature, such deviation must be related to superconducting pairing. As shown in Fig. S6(a) in the Supplemental Material [32], a clear shift of NMR spectrum to low frequency without any change of profile indicates an intrinsic suppression of the uniform spin susceptibility below 60 K. A similar deviation from high-temperature behavior is also observed in the temperature-dependent $1/T_1T$ [Fig. 2(b)], which is in agreement with the Knight shift results. Moreover, the temperature-dependent stretching exponent of T_1 fitting shown in Fig. S6(b) in the Supplemental Material [32]

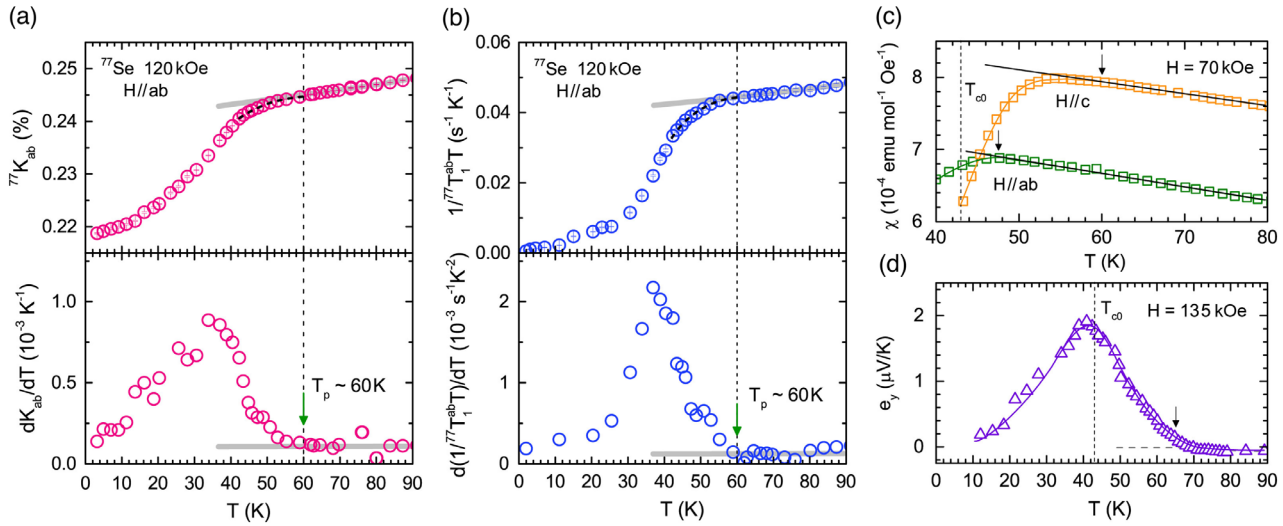

FIG. 2. Evidence for preformed Cooper pairs above T_{c0} in $(TBA)_xFeSe$. (a) Temperature dependence of Knight shift K (upper panel) and its first derivative (lower panel). (b) Temperature dependence of the spin-lattice relaxation rate divided by temperature $1/T_1T$ (upper panel) and its first derivative (lower panel). The external magnetic field of 120 kOe in (a) and (b) was applied within the ab plane. (c) The high-field magnetic susceptibility χ_{ab} and χ_c measured in field-cooling mode with the magnetic field of 70 kOe applied in plane (green) and out of plane (orange), respectively. The black solid lines are the extrapolation fitting curves of high-temperature behavior. The arrow indicates the onset of diamagnetism. (d) Temperature dependence of Nernst effect under a magnetic field of 135 kOe applied along c axis. A vortex-related Nernst signal is observed well above T_{c0}. The arrow shows the onset of the vortex-related Nernst effect at ~65 K. It should be noted that the T_p determined by Nernst effect is slightly higher than other probes, which suggests that the Nernst effect is more sensitive to detecting superconducting fluctuation.

verifies a homogeneous spin dynamics in NMR timescale above T_{c0}. Therefore, the present NMR results support an intrinsic pseudogap behavior with the characteristic temperature $T_p \sim 60$ K. It should be emphasized that the similar temperature-dependent behavior between Knight shift and $1/T_1T$ also confirms that the observed pseudogap behavior is from quasiparticles instead of spin fluctuations. As shown in Fig. S3(a) in the Supplemental Material [32], the in-plane conductance exhibits a clear enhancement below 60 K, which is consistent with a fluctuating superconductivity above T_{c0}. In addition, it should be pointed out that the observed pseudogap behavior in NMR measurement is independent of field orientation or strength (refer to Supplemental Material [32], Section I, for more details). These results are consistent with a preformed pairing scenario with considerable pairing gap suggested by STM measurement shown in Fig. 1(b).

However, whether the pseudogap behavior in NMR measurements can be unambiguously ascribed to the preformed pairing is not straightforward if there are other electronic instabilities such as charge or spin density wave. Here, in order to further clarify the nature of the pseudogap behavior below T_p, the bulk magnetization was measured with external magnetic field applied in plane and out of plane. Usually, the weak diamagnetic signal due to the preformed pairing can be detected by the bulk magnetization measurement [82]. As shown in Fig. 2(c), the high-field magnetization shows a weak diamagnetic signal well above T_{c0} under magnetic field applied along c axis. The onset temperature of the weak diamagnetic signal is around $T_p \sim 60$ K, perfectly consistent with the NMR results. It strongly confirms that a 2D superconducting fluctuation emerges below T_p, being similar to the single-layer FeSe film [83]. It is well known that the Nernst effect is another quite sensitive probe for superconducting fluctuations [5]. As shown in Fig. 2(d), a remarkable Nernst signal is observed above T_{c0} under an external magnetic field of 135 kOe applied along c axis. At higher temperature, the Nernst signal is very small and almost temperature independent. Below about 65 K, the Nernst signal shows a clear increase and then reaches a maximum around 40 K. Below 40 K, the Nernst signal continuously decreases. Such temperature dependence of Nernst effect was widely observed in the underdoped cuprate superconductors, and the Nernst signal well above T_{c0} is usually ascribed to the free vortex contribution (common Gaussian fluctuation only appears around T_{c0}) [5]. The Nernst effect further supports a persistent superconducting fluctuation above T_{c0}, consistent with the results of NMR and diamagnetism. In addition, the above results of anisotropic diamagnetism and Nernst effect also rule out the possible origin of band structure [84] or nematicity [85] to explain the NMR results.

As shown in Figs. 3(a) and 3(b), the anisotropy of resistivity between out of plane and in plane was measured. Compared to bulk FeSe, the value of anisotropy is enhanced by about 5 orders of magnitude, suggesting an intercalation-induced dimensional crossover from 3D to

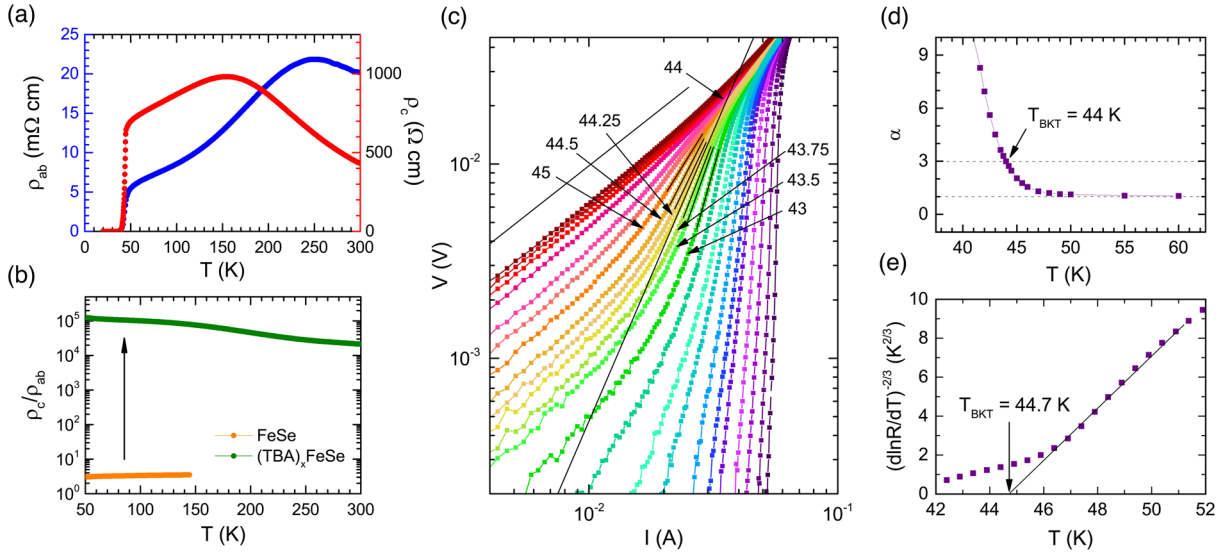

FIG. 3. Two-dimensional electronic properties of $(\mathrm{TBA})_x\mathrm{FeSe}$. (a) Temperature dependence of in-plane and out-of-plane resistivity. (b) The anisotropy of resistivity (ρ_c/ρ_{ab}) for $(\mathrm{TBA})_x\mathrm{FeSe}$ and pristine FeSe. The data of FeSe is adopted from Ref. [90]. (c) V (I) curves at various temperatures plotted in a logarithmic scale. The numbers provide the measured temperature for each curve. The short black lines are fits of the data across the T_{c0}. The two long black lines correspond to $V \sim I$ and $V \sim I^3$ behavior, respectively. The temperature for $V \sim I^3$ behavior is defined as $T_{\mathrm{BKT}} \sim 44$ K. (d) Temperature dependence of the power-law exponent α as deduced from the fits shown in (c). (e) R-T dependence for the $(\mathrm{TBA})_x\mathrm{FeSe}$ single crystal ($I = 500\ \mu$A) plotted in a $[d\ln(R)/dT]^{-2/3}$ scale. The solid line shows the fitting to the Halprin-Nelson formula $R(T) = R_0 \exp[-b/(T - T_{\mathrm{BKT}})^{1/2}]$ with $T_{\mathrm{BKT}} \sim 44.7$ K.

2D. Considering such highly 2D electronic structure, a natural explanation for the observed pseudogap behavior in these layered FeSe-based superconductors is related to strong phase fluctuations in 2D limit [24] in which the spontaneous topological excitations (vortex) due to strong phase fluctuations destroy the zero-resistance state below the 2D superconducting pairing temperature (T_c^{2D}). Based on the Berezinskii-Kosterlitz-Thouless (BKT) theory, the zero-resistance state only emerges when the vortex and antivortex are bound into pairs below a so-called BKT transition temperature (T_{BKT}) [86,87]. Such topological transition due to the unbinding of vortex-antivortex pairs manifests a jump of the power-law exponent in the current-voltage (I-V) characteristic curves and a disappearance of Ohmic resistance obeying the Halperin-Nelson scaling law [88], which are important manifestations of 2D superconductivity [89]. To further verify the nature of zero-resistance transition and pseudogap phenomenon, we carried out the measurement of temperature-dependent I-V curves across T_{c0}. As shown in Fig. 3(c), a power-law transition with $V \sim I^{\alpha}$ can be identified during the zero-resistance transition. We extracted the temperature dependence of the power-law exponent α, which was deduced by fitting the I-V curves, as shown in Fig. 3(d). At $T = 44$ K, the exponent α continuously approaches to the value of 3, which can be used to define a supposed BKT transition [89]. Moreover, the temperature-dependent resistance $R(T)$ follows a typical BKT-like behavior with $R(T) = R_0 \exp[-b/(T - T_{\mathrm{BKT}})^{1/2}]$ in the temperature range close to T_{BKT}, where R_0 and b are material dependent parameters [88]. As shown in Fig. 3(e), the extracted value of T_{BKT} from the measured $R(T)$ curve is about 44.7 K, which is in agreement with the I-V results. Both anisotropic transport and I-V curves evidently support a 2D-like (or BKT-like) nature in these layered FeSe-based superconductors, which hints at an important role for phase fluctuation.

Up to now, all experimental results obtained by different techniques support a pseudogap behavior due to the preformed pairing below $T_p \sim 60$ K and a highly anisotropic superconductivity below $T_{c0} \sim 43$ K in $(\mathrm{TBA})_x\mathrm{FeSe}$. A summarized H-T phase diagram is shown in Fig. 4. Here, we would like to emphasize that vortex physics might be more sophisticated if considering a role of quenched disorder on the vortex dynamics, but it is not the focus in the present study. We leave this issue of detailed vortex physics to future work. The similar pseudogap behavior is also observed in another layered FeSe-based superconductor $(\mathrm{CTA})_x\mathrm{FeSe}$ (refer to Supplemental Material [32], Section II, for more details). These results confirm that such a pseudogap behavior is intrinsic for the layered FeSe-based superconductors. In addition, STM measurement indicates that the local superconducting gap is about 16 meV in these layered FeSe-based superconductors [see Fig. 1(b) for $(\mathrm{TBA})_x\mathrm{FeSe}$ and Fig. S10 in Supplemental Material [32], Section II, for $(\mathrm{CTA})_x\mathrm{FeSe}$], which is comparable to that of the single-layer FeSe film with the gap value varying from 13 to 20 meV (see Fig. S11 in

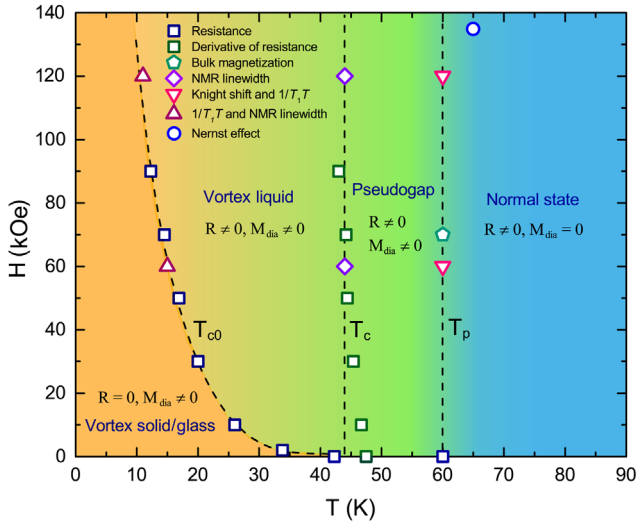

FIG. 4. Summarized H-T phase diagram for $(TBA)_xFeSe$. The external magnetic field is parallel to the c axis. T_{c0} stands for zero-resistance transition temperature, which is also consistent with the T_m defined by NMR measurement under magnetic field. T_c stands for the superconducting temperature defined by the onset temperature of NMR line broadening and the first derivative of resistance data. T_p stands for the onset temperature of pseudogap behavior. Resistivity, magnetization, and NMR measurements give the same T_p of about 60 K, while the Nernst effect gives a slightly higher T_p of about 65 K. It suggests that Nernst effect is more sensitive than other probes to detecting superconducting fluctuations. In the vortex solid or vortex glass state, the resistivity becomes zero with highly anisotropic diamagnetism. In the vortex liquid state, the resistivity is no longer zero but there is still anisotropic diamagnetic signal. Such phase diagram for vortex is similar to that of high-T_c cuprate superconductors [35] in which the vortex physics is strongly affected by the 2D superconducting fluctuations. Above T_c, a remarkable pseudogap phenomenon appears up to T_p.

Section III of the Supplemental Material [32]). Therefore, the much higher pairing temperature (~65 K) compared to zero-resistance transition temperature (< 40 K) in the single-layer FeSe film might be also ascribed to the same preformed pairing scenario. These works indicate that strong phase fluctuation is an important character in 2D iron-based superconductors as widely observed in high-T_c cuprate superconductors. How to understand the underlying physics behind preformed pairing is relevant to high-T_c mechanism and brings a challenge to theory. To summarize, our work not only reveals the preformed Cooper pairs but also suggests a possible enhancement of pairing strength by dimensional crossover from 3D to 2D.

We thank Z. J. Xiang for valuable suggestions on Nernst measurement and F. C. Zhang and Z. Y. Weng for insightful discussion. This work is supported by the National Natural Science Foundation of China (Grants No. 11888101, No. 11522434), the National Key R&D Program of the MOST of China (Grants No. 2016YFA0300201, No. 2017YFA0303000), the Strategic Priority Research Program of Chinese Academy of Sciences (Grant No. XDB25000000), and the Anhui Initiative in Quantum Information Technologies (Grant No. AHY160000).

B. L. K. and M. Z. S. contributed equally to this work.

*Corresponding author.
wutao@ustc.edu.cn
†Corresponding author.
chenxh@ustc.edu.cn

[1] V. J. Emery and S. A. Kivelson, Importance of phase fluctuations in superconductors with small superfluid density, Nature (London) **374**, 434 (1995).
[2] P. A. Lee, N. Nagaosa, and X. G. Wen, Doping a Mott insulator: Physics of high-temperature superconductivity, Rev. Mod. Phys. **78**, 17 (2006).
[3] Y. J. Uemura *et al.*, Universal Correlations Between T_c and n_s/m^* (Carrier Density Over Effective Mass) in High-T_c Cuprate Superconductors, Phys. Rev. Lett. **62**, 2317 (1989).
[4] L. Li, Y. Y. Wang, S. Komiya, S. Ono, Y. Ando, G. D. Gu, and N. P. Ong, Diamagnetism and Cooper pairing above T_c in cuprates, Phys. Rev. B **81**, 054510 (2010).
[5] Y. Y. Wang, L. Li, and N. P. Ong, Nernst effect in high-T_c superconductors, Phys. Rev. B **73**, 024510 (2006).
[6] J. L. Tallon, J. G. Storey, and J. W. Loram, Fluctuations and critical temperature reduction in cuprate superconductors, Phys. Rev. B **83**, 092502 (2011).
[7] J. Corson, R. Mallozzi, J. Orenstein, J. N. Eckstein, and I. Bozovic, Vanishing of phase coherence in underdoped $Bi_2Sr_2CaCu_2O_{8+\delta}$, Nature (London) **398**, 221 (1999).
[8] S. Kasahara, T. Yamashita, A. Shi, R. Kobayashi, Y. Shimoyama, T. Watashige, K. Ishida, T. Terashima, T. Wolf, F. Hardy, C. Meingast, H. Von Lohneysen, A. Levchenko, T. Shibauchi, and Y. Matsuda, Giant superconducting fluctuations in the compensated semimetal FeSe at the BCS-BEC crossover, Nat. Commun. **7**, 12843 (2016).
[9] H. Takahashi, F. Nabeshima, R. Ogawa, E. Ohmichi, H. Ohta, and A. Maeda, Superconducting fluctuations in FeSe investigated by precise torque magnetometry, Phys. Rev. B **99**, 060503 (2019).
[10] K. Ahilan, F. L. Ning, T. Imai, A. S. Sefat, R. Jin, M. A. McGuire, B. C. Sales, and D. Mandrus, ^{19}F NMR investigation of the iron pnictide superconductor $LaFeAsO_{0.89}F_{0.11}$, Phys. Rev. B **78**, 100501 (2008).
[11] T. Sato, S. Souma, K. Nakayama, K. Terashima, K. Sugawara, T. Takahashi, Y. Kamihara, M. Hirano, and H. Hosono, Superconducting gap and pseudogap in iron-based layered superconductor $La(O_{1-x}F_x)FeAs$, J. Phys. Soc. Jpn. **77**, 063708 (2008).
[12] Z. W. Zhu, Z. A. Xu, X. Lin, G. H. Cao, C. M. Feng, G. F. Chen, Z. Li, J. L. Luo, and N. L. Wang, Nernst effect of a new iron-based superconductor $LaO_{1-x}F_xFeAs$, New J. Phys. **10**, 063021 (2008).
[13] A. L. Shi, T. Arai, S. Kitagawa, T. Yamanaka, K. Ishida, A. E. Bohmer, C. Meingast, T. Wolf, M. Hirata, and T. Sasaki, Pseudogap behavior of the nuclear spin-lattice

relaxation rate in FeSe probed by ^{77}Se NMR, J. Phys. Soc. Jpn. **87**, 013704 (2018).

[14] Q. Y. Wang, Z. Li, W. H. Zhang, Z. C. Zhang, J. S. Zhang, W. Li, H. Ding, Y. B. Ou, P. Deng, K. Chang, J. Wen, C. L. Song, K. He, J. F. Jia, S. H. Ji, Y. Y. Wang, L. L. Wang, X. Chen, X. C. Ma, and Q. K. Xue, Interface-induced high-temperature superconductivity in single unit-cell FeSe films on $SrTiO_3$, Chin. Phys. Lett. **29**, 037402 (2012).

[15] J. J. Lee, F. T. Schmitt, R. G. Moore, S. Johnston, Y. T. Cui, W. Li, M. Yi, Z. K. Liu, M. Hashimoto, Y. Zhang, D. H. Lu, T. P. Devereaux, D. H. Lee, and Z. X. Shen, Interfacial mode coupling as the origin of the enhancement of T_c in FeSe films on $SrTiO_3$, Nature (London) **515**, 245 (2014).

[16] D. H. Lee, What makes the T_c of FeSe/$SrTiO_3$ so high, Chin. Phys. B **24**, 117405 (2015).

[17] Y. Miyata, K. Nakayama, K. Sugawara, T. Sato, and T. Takahashi, High-temperature superconductivity in potassium-coated multilayer FeSe thin films, Nat. Mater. **14**, 775 (2015).

[18] L. Rademaker, Y. Wang, T. Berlijn, and S. Johnston, Enhanced superconductivity due to forward scattering in FeSe thin films on $SrTiO_3$ substrates, New J. Phys. **18**, 022001 (2016).

[19] Y. J. Zhou and A. J. Millis, Dipolar phonons and electronic screening in monolayer FeSe on $SrTiO_3$, Phys. Rev. B **96**, 054516 (2017).

[20] Q. Song, T. L. Yu, X. Lou, B. P. Xie, H. C. Xu, C. H. P. Wen, Q. Yao, S. Y. Zhang, X. T. Zhu, J. D. Guo, R. Peng, and D. L. Feng, Evidence of cooperative effect on the enhanced superconducting transition temperature at the FeSe/$SrTiO_3$ interface, Nat. Commun. **10**, 758 (2019).

[21] F. M. Li and G. A. Sawatzky, Electron Phonon Coupling Versus Photoelectron Energy Loss at the Origin of Replica Bands in Photoemission of FeSe on $SrTiO_3$, Phys. Rev. Lett. **120**, 237001 (2018).

[22] S. L. He *et al.*, Phase diagram and electronic indication of high-temperature superconductivity at 65 K in single-layer FeSe films, Nat. Mater. **12**, 605 (2013).

[23] S. Y. Tan, Y. Zhang, M. Xia, Z. R. Ye, F. Chen, X. Xie, R. Peng, D. F. Xu, Q. Fan, H. C. Xu, J. Jiang, T. Zhang, X. C. Lai, T. Xiang, J. P. Hu, B. P. Xie, and D. L. Feng, Interface-induced superconductivity and strain-dependent spin density waves in FeSe/$SrTiO_3$ thin films, Nat. Mater. **12**, 634 (2013).

[24] W. H. Zhang *et al.*, Direct Observation of high-temperature superconductivity in one-unit-cell FeSe films, Chin. Phys. Lett. **31**, 017401 (2014).

[25] W. H. Zhang, Z. Li, F. S. Li, H. M. Zhang, J. P. Peng, C. J. Tang, Q. Y. Wang, K. He, X. Chen, L. L. Wang, X. C. Ma, and Q. K. Xue, Interface charge doping effects on superconductivity of single-unit-cell FeSe films on $SrTiO_3$ substrates, Phys. Rev. B **89**, 060506 (2014).

[26] Y. Sun, W. H. Zhang, Y. Xing, F. S. Li, Y. F. Zhao, Z. C. Xia, L. L. Wang, X. C. Ma, Q. K. Xue, and J. Wang, High temperature superconducting FeSe films on $SrTiO_3$ substrates, Sci. Rep. **4**, 6040 (2014).

[27] Q. Y. Wang, W. H. Zhang, Z. C. Zhang, Y. Sun, Y. Xing, Y. Y. Wang, L. L. Wang, X. C. Ma, Q. K. Xue, and J. Wang, Thickness dependence of superconductivity and superconductor-insulator transition in ultrathin FeSe films on $SrTiO_3$ (001) substrate, 2D Mater. **2**, 044012 (2015).

[28] M. Z. Shi, N. Z. Wang, B. Lei, C. Shang, F. B. Meng, L. K. Ma, F. X. Zhang, D. Z. Kuang, and X. H. Chen, Organic-ion-intercalated FeSe-based superconductors, Phys. Rev. Mater. **2**, 074801 (2018).

[29] M. Z. Shi, N. Z. Wang, B. Lei, J. J. Ying, C. S. Zhu, Z. L. Sun, J. H. Cui, F. B. Meng, C. Shang, L. K. Ma, and X. H. Chen, FeSe-based superconductors with a superconducting transition temperature of 50 K, New J. Phys. **20**, 123007 (2018).

[30] B. Lei, J. H. Cui, Z. J. Xiang, C. Shang, N. Z. Wang, G. J. Ye, X. G. Luo, T. Wu, Z. Sun, and X. H. Chen, Evolution of High-Temperature Superconductivity from a Low-T_c Phase Tuned by Carrier Concentration in FeSe Thin Flakes, Phys. Rev. Lett. **116**, 077002 (2016).

[31] C. Berthier, M. H. Julien, M. Horvatic, and Y. Berthier, NMR studies of the normal state of high temperature superconductors, J. Phys. I (France) **6**, 2205 (1996).

[32] See Supplemental Material at http://link.aps.org/supplemental/10.1103/PhysRevLett.125.097003 for details of experimental methods and additional measurement data, which includes Refs. [14,15,17,22–25,28,29,33–79].

[33] D. Chareev, E. Osadchii, T. Kuzmicheva, J. Y. Lin, S. Kuzmichev, O. Volkova, and A. Vasiliev, Single crystal growth and characterization of tetragonal $FeSe_{1-x}$ superconductors, CrystEngComm **15**, 1989 (2013).

[34] S. L. Budko, N. Ni, and P. C. Canfield, Jump in specific heat at the superconducting transition temperature in $Ba(Fe_{1-x}Co_x)_2As_2$ and $Ba(Fe_{1-x}Ni_x)_2As_2$ single crystals, Phys. Rev. B **79**, 220516 (2009).

[35] G. Blatter, M. V. Feigelman, V. B. Geshkenbein, A. I. Larkin, and V. M. Vinokur, Vortices in high-temperature superconductors, Rev. Mod. Phys. **66**, 1125 (1994).

[36] S. H. Baek, H. J. Grafe, F. Hammerath, M. Fuchs, C. Rudisch, L. Harnagea, S. Aswartham, S. Wurmehl, J. van den Brink, and B. Buchner, ^{75}As NMR-NQR study in superconducting LiFeAs, Eur. Phys. J. B **85**, 159 (2012).

[37] Z. Li, J. P. Peng, H. M. Zhang, W. H. Zhang, H. Ding, P. Deng, K. Chang, C. L. Song, S. H. Ji, L. L. Wang, K. He, X. Chen, Q. K. Xue, and X. C. Ma, Molecular beam epitaxy growth and post-growth annealing of FeSe films on $SrTiO_3$: A scanning tunneling microscopy study, J. Phys. Condens. Matter **26**, 265002 (2014).

[38] C. L. Song, Y. L. Wang, P. Cheng, Y. P. Jiang, W. Li, T. Zhang, Z. Li, K. He, L. L. Wang, J. F. Jia, H. H. Hung, C. J. Wu, X. C. Ma, X. Chen, and Q. K. Xue, Direct observation of nodes and twofold symmetry in FeSe superconductor, Science **332**, 1410 (2011).

[39] S. Kasahara, T. Watashige, T. Hanaguri, Y. Kohsaka, T. Yamashita, Y. Shimoyama, Y. Mizukami, R. Endo, H. Ikeda, K. Aoyama, T. Terashima, S. Uji, T. Wolf, H. von Lohneysen, T. Shibauchi, and Y. Matsuda, Field-induced superconducting phase of FeSe in the BCS-BEC crossover, Proc. Natl. Acad. Sci. U.S.A. **111**, 16309 (2014).

[40] P. Cai, C. Ye, W. Ruan, X. D. Zhou, A. F. Wang, M. Zhang, X. H. Chen, and Y. Y. Wang, Imaging the coexistence of a superconducting phase and a charge-density modulation in the $K_{0.73}Fe_{1.67}Se_2$ superconductor using a scanning tunneling microscope, Phys. Rev. B **85**, 094512 (2012).

[41] L. Zhao *et al.*, Common Fermi-surface topology and nodeless superconducting gap of $K_{0.68}Fe_{1.79}Se_2$ and $(Tl_{0.45}K_{0.34})Fe_{1.84}Se_2$ superconductors revealed via angle-resolved photoemission, Phys. Rev. B **83**, 140508 (2011).

[42] X. P. Wang, T. Qian, P. Richard, P. Zhang, J. Dong, H. D. Wang, C. H. Dong, M. H. Fang, and H. Ding, Strong nodeless pairing on separate electron Fermi surface sheets in $(Tl, K)Fe_{1.78}Se_2$ probed by ARPES, Europhys. Lett. **93**, 57001 (2011).

[43] Y. Zhang, L. X. Yang, M. Xu, Z. R. Ye, F. Chen, C. He, H. C. Xu, J. Jiang, B. P. Xie, J. J. Ying, X. F. Wang, X. H. Chen, J. P. Hu, M. Matsunami, S. Kimura, and D. L. Feng, Nodeless superconducting gap in $A_xFe_2Se_2(A = K, Cs)$ revealed by angle-resolved photoemission spectroscopy, Nat. Mater. **10**, 273 (2011).

[44] D. X. Mou *et al.*, Distinct Fermi Surface Topology and Nodeless Superconducting Gap in a $(Tl_{0.58}Rb_{0.42})Fe_{1.72}Se_2$ Superconductor, Phys. Rev. Lett. **106**, 107001 (2011).

[45] X. H. Niu, R. Peng, H. C. Xu, Y. J. Yan, J. Jiang, D. F. Xu, T. L. Yu, Q. Song, Z. C. Huang, Y. X. Wang, B. P. Xie, X. F. Lu, N. Z. Wang, X. H. Chen, Z. Sun, and D. L. Feng, Surface electronic structure and isotropic superconducting gap in $(Li_{0.8}Fe_{0.2})$OHFeSe, Phys. Rev. B **92**, 060504 (2015).

[46] R. Khasanov, H. X. Zhou, A. Amato, Z. Guguchia, E. Morenzoni, X. L. Dong, G. M. Zhang, and Z. X. Zhao, Proximity-induced superconductivity within the insulating $(Li_{0.84}Fe_{0.16})$OH layers in $(Li_{0.84}Fe_{0.16})$OH$Fe_{0.98}$Se, Phys. Rev. B **93**, 224512 (2016).

[47] L. Zhao *et al.*, Common electronic origin of superconductivity in (Li,Fe)OHFeSe bulk superconductor and single-layer FeSe/$SrTiO_3$ films, Nat. Commun. **7**, 10608 (2016).

[48] M. W. Ma, L. C. Wang, P. Bourges, Y. Sidis, S. Danilkin, and Y. Li, Low-energy spin excitations in $(Li_{0.8}Fe_{0.2})$ODFeSe superconductor studied with inelastic neutron scattering, Phys. Rev. B **95**, 100504 (2017).

[49] Z. Y. Du, X. Yang, H. Lin, D. L. Fang, G. Du, J. Xing, H. Yang, X. Y. Zhu, and H. H. Wen, Scrutinizing the double superconducting gaps and strong coupling pairing in $(Li_{1-x}Fe_x)$OHFeSe, Nat. Commun. **7**, 10565 (2016).

[50] M. Q. Ren, Y. J. Yan, X. H. Niu, R. Tao, D. Hu, R. Peng, B. P. Xie, J. Zhao, T. Zhang, and D. L. Feng, Superconductivity across Lifshitz transition and anomalous insulating state in surface K-dosed $(Li_{0.8}Fe_{0.2}OH)$FeSe, Sci. Adv. **3**, e1603238 (2017).

[51] Y. J. Yan, W. H. Zhang, M. Q. Ren, X. Liu, X. F. Lu, N. Z. Wang, X. H. Niu, Q. Fan, J. Miao, R. Tao, B. P. Xie, X. H. Chen, T. Zhang, and D. L. Feng, Surface electronic structure and evidence of plain s-wave superconductivity in $(Li_{0.8}Fe_{0.2})$OHFeSe, Phys. Rev. B **94**, 134502 (2016).

[52] D. Huang, C. L. Song, T. A. Webb, S. Fang, C. Z. Chang, J. S. Moodera, E. Kaxiras, and J. E. Hoffman, Revealing the Empty-State Electronic Structure of Single-Unit-Cell FeSe/$SrTiO_3$, Phys. Rev. Lett. **115**, 017002 (2015).

[53] D. F. Liu *et al.*, Electronic origin of high-temperature superconductivity in single-layer FeSe superconductor, Nat. Commun. **3**, 931 (2012).

[54] F. C. Hsu, J. Y. Luo, K. W. Yeh, T. K. Chen, T. W. Huang, P. M. Wu, Y. C. Lee, Y. L. Huang, Y. Y. Chu, D. C. Yan, and M. K. Wu, Superconductivity in the PbO-type structure α-FeSe, Proc. Natl. Acad. Sci. U.S.A. **105**, 14262 (2008).

[55] K. W. Yeh, T. W. Huang, Y. L. Huang, T. K. Chen, F. C. Hsu, P. M. Wu, Y. C. Lee, Y. Y. Chu, C. L. Chen, J. Y. Luo, D. C. Yan, and M. K. Wu, Tellurium substitution effect on superconductivity of the α-phase iron selenide, Europhys. Lett. **84**, 37002 (2008).

[56] J. G. Guo, H. C. Lei, F. Hayashi, and H. Hosono, Superconductivity and phase instability of NH_3-free Na-intercalated $FeSe_{1-z}S_z$, Nat. Commun. **5**, 4756 (2014).

[57] T. Kajita, T. Kawamata, T. Noji, T. Hatakeda, M. Kato, Y. Koike, and T. Itoh, Electrochemical Na-intercalation-induced high-temperature superconductivity in FeSe, Physica (Amsterdam) **519C**, 104 (2015).

[58] M. H. Fang, H. D. Wang, C. H. Dong, Z. J. Li, C. M. Feng, J. Chen, and H. Q. Yuan, Fe-based superconductivity with $T_c = 31$ K bordering an antiferromagnetic insulator in $(Tl, K)Fe_xSe_2$, Europhys. Lett. **94**, 27009 (2011).

[59] A. M. Zhang, T. L. Xia, K. Liu, W. Tong, Z. R. Yang, and Q. M. Zhang, Superconductivity at 44 K in K intercalated FeSe system with excess Fe, Sci. Rep. **3**, 1216 (2013).

[60] A. F. Wang, J. J. Ying, Y. J. Yan, R. H. Liu, X. G. Luo, Z. Y. Li, X. F. Wang, M. Zhang, G. J. Ye, P. Cheng, Z. J. Xiang, and X. H. Chen, Superconductivity at 32 K in single-crystalline $Rb_xFe_{2-y}Se_2$, Phys. Rev. B **83**, 060512 (2011).

[61] T. P. Ying, X. L. Chen, G. Wang, S. F. Jin, X. F. Lai, T. T. Zhou, H. Zhang, S. J. Shen, and W. Y. Wang, Superconducting phases in potassium-intercalated iron selenides, J. Am. Chem. Soc. **135**, 2951 (2013).

[62] A. Krzton-Maziopa, Z. Shermadini, E. Pomjakushina, V. Pomjakushin, M. Bendele, A. Amato, R. Khasanov, H. Luetkens, and K. Conder, Synthesis and crystal growth of $Cs_{0.8}(FeSe_{0.98})_2$: A new iron-based superconductor with $T_c = 27$ K, J. Phys. Condens. Matter **23**, 052203 (2011).

[63] L. Zheng, M. Izumi, Y. Sakai, R. Eguchi, H. Goto, Y. Takabayashi, T. Kambe, T. Onji, S. Araki, T. C. Kobayashi, J. Kim, A. Fujiwara, and Y. Kubozono, Superconductivity in $(NH_3)_yCs_{0.4}$FeSe, Phys. Rev. B **88**, 094521 (2013).

[64] M. Burrard-Lucas, D. G. Free, S. J. Sedlmaier, J. D. Wright, S. J. Cassidy, Y. Hara, A. J. Corkett, T. Lancaster, P. J. Baker, S. J. Blundell, and S. J. Clarke, Enhancement of the superconducting transition temperature of FeSe by intercalation of a molecular spacer layer, Nat. Mater. **12**, 15 (2013).

[65] E. W. Scheidt, V. R. Hathwar, D. Schmitz, A. Dunbar, W. Scherer, F. Mayr, V. Tsurkan, J. Deisenhofer, and A. Loidl, Superconductivity at $T_c = 44$ K in $Li_xFe_2Se_2(NH_3)_y$, Eur. Phys. J. B **85**, 279 (2012).

[66] K. V. Yusenko, J. Sottmann, H. Emerich, W. A. Crichton, L. Malavasi, and S. Margadonna, Hyper-expanded interlayer separations in superconducting barium intercalates of FeSe, Chem. Commun. (Cambridge) **51**, 7112 (2015).

[67] T. P. Ying, X. L. Chen, G. Wang, S. F. Jin, T. T. Zhou, X. F. Lai, H. Zhang, and W. Y. Wang, Observation of superconductivity at 30 K ~ 46 K in $A_xFe_2Se_2$ (A = Li, Na, Ba, Sr, Ca, Yb, and Eu), Sci. Rep. **2**, 426 (2012).

[68] F. R. Foronda, S. Ghannadzadeh, S. J. Sedlmaier, J. D. Wright, K. Burns, S. J. Cassidy, P. A. Goddard, T. Lancaster, S. J. Clarke, and S. J. Blundell, Robustness of superconductivity to structural disorder in $Sr_{0.3}(NH_2)_y(NH_3)_{1-y}Fe_2Se_2$, Phys. Rev. B **92**, 134517 (2015).

[69] F. Hayashi, H. C. Lei, J. G. Guo, and H. Hosono, Modulation effect of interlayer spacing on the superconductivity of electron-doped FeSe-based intercalates, Inorg. Chem. **54**, 3346 (2015).

[70] L. Zheng, X. Miao, Y. Sakai, M. Izumi, H. Goto, S. Nishiyama, E. Uesugi, Y. Kasahara, Y. Iwasa, and Y. Kubozono, Emergence of Multiple Superconducting Phases in $(NH_3)_yM_xFeSe$ (M: Na and Li), Sci. Rep. **5**, 12774 (2015).

[71] X. F. Lu, N. Z. Wang, H. Wu, Y. P. Wu, D. Zhao, X. Z. Zeng, X. G. Luo, T. Wu, W. Bao, G. H. Zhang, F. Q. Huang, Q. Z. Huang, and X. H. Chen, Coexistence of superconductivity and antiferromagnetism in $(Li_{0.8}Fe_{0.2})$OHFeSe, Nat. Mater. **14**, 325 (2015).

[72] S. J. Shen, T. P. Ying, G. Wang, S. F. Jin, H. Zhang, Z. P. Lin, and X. L. Chen, Electro-chemical synthesis of alkali-intercalated iron selenide superconductors, Chin. Phys. B **24**, 117406 (2015).

[73] S. F. Jin, X. Fan, X. Z. Wu, R. J. Sun, H. Wu, Q. Z. Huang, C. L. Shi, X. K. Xi, Z. L. Li, and X. L. Chen, High-T_c superconducting phases in organic molecular intercalated iron selenides: Synthesis and crystal structures, Chem. Commun. (Cambridge) **53**, 9729 (2017).

[74] S. Hosono, T. Noji, T. Hatakeda, T. Kawamata, M. Kato, and Y. Koike, New superconducting phase of $Li_x(C_6H_{16}N_2)_yFe_{2-z}Se_2$ with $T_c = 41$ K obtained through the post-annealing, J. Phys. Soc. Jpn. **85**, 013702 (2016).

[75] H. S. Xu, X. X. Wang, Z. Gao, H. L. Huang, Y. Z. Long, Y. L. Lu, and K. B. Tang, New alkali-metal and 1,2-diaminopropane intercalated superconductor $Li_x(C_3H_{10}N_2)_yFe_2Se_2$ with $T_c = 45$ K, J. Alloys Compd. **735**, 2053 (2018).

[76] A. Krzton-Maziopa, E. V. Pomjakushina, V. Y. Pomjakushin, F. von Rohr, A. Schilling, and K. Conder, Synthesis of a new alkali metal-organic solvent intercalated iron selenide superconductor with T_c approximate to 45 K, J. Phys. Condens. Matter **24**, 382202 (2012).

[77] S. Hosono, T. Noji, T. Hatakeda, T. Kawamata, M. Kato, and Y. Koike, New intercalation superconductor $Li_x(C_6H_{16}N_2)_yFe_{2-z}Se_2$ with a very large interlayer-spacing and $T_c = 38$ K, J. Phys. Soc. Jpn. **83**, 113704 (2014).

[78] T. Hatakeda, T. Noji, K. Sato, T. Kawamata, M. Kato, and Y. Koike, New alkali-metal- and 2-phenethylamine-intercalated superconductors $A_x(C_8H_{11}N)_yFe_{1-z}Se$ (A = Li, Na) with the largest interlayer spacings and T_c similar to 40 K, J. Phys. Soc. Jpn. **85**, 103702 (2016).

[79] J. Shiogai, Y. Ito, T. Mitsuhashi, T. Nojima, and A. Tsukazaki, Electric-field-induced superconductivity in electrochemically etched ultrathin FeSe films on $SrTiO_3$ and MgO, Nat. Phys. **12**, 42 (2016).

[80] J. Korringa, Nuclear magnetic relaxation and resonance line shift in metals, Physica (Amsterdam) **16**, 601 (1950).

[81] H. Alloul, T. Ohno, and P. Mendels, ^{89}Y NMR Evidence for a Fermi-Liquid Behavior in $YBa_2Cu_3O_{6+x}$, Phys. Rev. Lett. **63**, 1700 (1989).

[82] Q. Li, M. Hucker, G. D. Gu, A. M. Tsvelik, and J. M. Tranquada, Two-Dimensional Superconducting Fluctuations in Stripe-Ordered $La_{1.875}Ba_{0.125}CuO_4$, Phys. Rev. Lett. **99**, 067001 (2007).

[83] Z. C. Zhang, Y. H. Wang, Q. Song, C. Liu, R. Peng, K. A. Moler, D. L. Feng, and Y. Y. Wang, Onset of the Meissner effect at 65 K in FeSe thin film grown on Nb-doped $SrTiO_3$ substrate, Sci. Bull. **60**, 1301 (2015).

[84] H. Ikeda, R. Arita, and J. Kunes, Doping dependence of spin fluctuations and electron correlations in iron pnictides, Phys. Rev. B **82**, 024508 (2010).

[85] S. H. Baek, D. V. Efremov, J. M. Ok, J. S. Kim, J. van den Brink, and B. Buchner, Orbital-driven nematicity in FeSe, Nat. Mater. **14**, 210 (2015).

[86] V. L. Berezinskii, Destruction of long-range order in one-dimensional and two-dimensional systems having a continuous symmetry group I. Classical Systems, Sov. Phys. JETP **32**, 493 (1971); II. Quantum Systems, Sov. Phys. JETP **34**, 610 (1972).

[87] J. M. Kosterlitz and D. J. Thouless, Ordering, metastability and phase-transitions in two dimensional systems, J. Phys. C **6**, 1181 (1973).

[88] B. I. Halperin and D. R. Nelson, Resistive transition in superconducting films, J. Low Temp. Phys. **36**, 599 (1979).

[89] N. Reyren, S. Thiel, A. D. Caviglia, L. F. Kourkoutis, G. Hammerl, C. Richter, C. W. Schneider, T. Kopp, A. S. Ruetschi, D. Jaccard, M. Gabay, D. A. Muller, J. M. Triscone, and J. Mannhart, Superconducting interfaces between insulating oxides, Science **317**, 1196 (2007).

[90] S. I. Vedeneev, B. A. Piot, D. K. Maude, and A. V. Sadakov, Temperature dependence of the upper critical field of FeSe single crystals, Phys. Rev. B **87**, 134512 (2013).